

Planar defects in a precursor for phosphor materials: $\text{SrAl}_2 - x\text{B}_x\text{O}_4$ ($x < 0.2$)

M. L. Ruiz-González,^a J. M. González-Calbet,^a M. Vallet-Regí,^{*b} E. Cordoncillo,^c P. Escribano,^c J. B. Carda^c and M. Marchal^c

^aDpto. Química Inorgánica, Facultad de Química, Universidad Complutense, 28040 Madrid, Spain

^bDpto. Química Inorgánica y Bioinorgánica, Facultad de Farmacia, Universidad Complutense, 28040 Madrid, Spain. Tel: 34 91 394 18 43; Fax: 34 91 394 17 86;

E-mail: vallet@farm.ucm.es

^cDpto. de Química Inorgánica y Orgánica, Universitat Jaume I, 12080 Castellón, Spain

Received 28th November 2001, Accepted 21st January 2002

First published as an Advance Article on the web 19th February 2002

The synthesis and structural characterization of a new precursor solid solution $\text{SrAl}_2 - x\text{B}_x\text{O}_4$ ($0 < x < 0.2$), for phosphor materials is reported. The synthesis temperature of SrAl_2O_4 is considerably reduced by B substitution. The new solid solution keeps the tridymite-like structure ($P2_1$) characteristic of SrAl_2O_4 . Microstructural characterization, by means of SAED and HREM, did not evidence additional ordering due to B doping. However, damage under the electron beam gives rise to complex defects, suggesting that B substitutes Al at tetrahedral positions in isolated planes along the [011] direction.

Introduction

Phosphors based on MAl_2O_4 ($\text{M} = \text{Ca}, \text{Sr}, \text{Ba}$)¹ have been widely studied in the last two decades due to applications such as hosts for ceramic pigments, practical phosphors and excitation sources for other phosphors and luminous paints. Moreover, doping with a rare-earth has had great relevance on the optimization of the properties of luminescence materials. In this sense, Eu-doped strontium aluminate² shows a long lasting phosphorescence and high brightness phenomenon.

SrAl_2O_4 has the tridymite-like structure.³ The parent structure corresponds to a SiO_2 polymorph, built up of $[\text{SiO}_4]$ tetrahedral layers sharing corners, giving rise to six corner rings, as depicted in Fig. 1. Aluminium occupies silicon sites in the SrAl_2O_4 material while strontium occupies the hexagonal holes leading to a lattice distortion and then to lower symmetry. Moreover, SrAl_2O_4 displays two polymorphic forms: (i) below 650 °C, it exhibits monoclinic symmetry ($P2_1$) and (ii) above this temperature it turns into hexagonal ($P6_322$). Such a transition is a displacive⁴ one, since it does not involve breaking of bonds only changes in the tetrahedra

orientation. A similar transition happens between the α and β forms of SiO_2 .⁵

The $\text{SrO-Al}_2\text{O}_3$ phase diagram shows that synthesis of SrAl_2O_4 , by the conventional ceramic method, requires temperatures above 1900 °C. To reduce such a synthesis temperature the addition of B_2O_3 as a fundent has been proved to be successful.⁶

Having taken into account the above ideas, we describe in this paper the optimization of the synthetic conditions at low temperature of B-doped SrAl_2O_4 and its microstructural characterization in comparison to SrAl_2O_4 .

Experimental

Samples with a nominal composition $\text{SrAl}_2 - x\text{B}_x\text{O}_4$ ($x = 0, 0.1$ and 0.2) were prepared from stoichiometric amounts of SrCO_3 , Al_2O_3 and H_3BO_3 . The mixture was ground in a planetary ball mill for 20 min and fired in an electrical furnace at different temperatures, 1100, 1200, 1300, 1400 and 1500 °C, with soaking times of 1 and 10 h at each temperature.

Phase evolution was carried out by powder X-ray diffraction (XRD) in a Siemens D-5000 diffractometer with $\text{Cu K}\alpha$ radiation. Boron was analysed by inductive coupled plasma (ICP) spectroscopy. Microstructural characterization, by means of electron diffraction (SAED) and high resolution electron microscopy (HREM), was performed on both JEOL 2000 FX and JEOL 4000 EX electron microscopes.

Results and discussion

The XRD study shows that temperatures above 1500 °C are required to obtain the monoclinic SrAl_2O_4 polymorph as a single phase with unit cell parameters: $a = 8.442(2)$ Å, $b = 8.822(2)$ Å, $c = 5.161(3)$ Å, $\beta = 93.42(2)^\circ$ and space group $P2_1$, in agreement with previous data.⁷ However, when different quantities of boron are added, the synthesis temperature is considerably reduced and the monoclinic phase is obtained at 1200 °C for a $\text{SrAl}_{1.8}\text{B}_{0.2}\text{O}_4$ nominal composition.

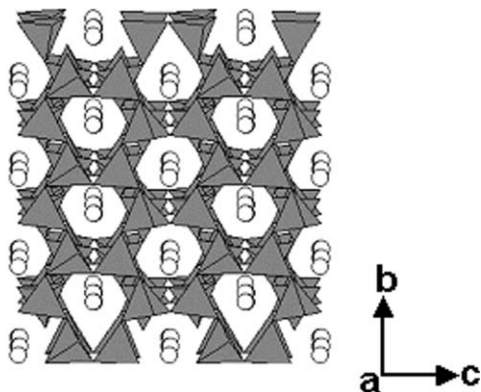


Fig. 1 Tridymite structure projected along [100].

No extra peaks are observed in the XRD pattern with respect to the undoped sample. A very slight decrease of the unit cell parameters for $\text{SrAl}_{1.8}\text{B}_{0.2}\text{O}_4$ is observed, $a = 8.439(3) \text{ \AA}$, $b = 8.818(2) \text{ \AA}$, $c = 5.153(2) \text{ \AA}$, $\beta = 93.386(2)^\circ$, as a consequence of the smaller ionic radius of B.⁸ Doping with $x = 0.1$ also leads to the stabilization of the monoclinic phase although $T = 1400 \text{ }^\circ\text{C}$ is required to stabilize $\text{SrAl}_2 - x\text{B}_x\text{O}_4$ as a single phase. Higher B concentrations lead to sample vitrification. Chemical compositions, as determined by ICP, are in agreement with the nominal ones. Obviously, although the synthesis temperature has been dramatically reduced, analysis by ICP does not prove B has entered into the tridymite structure since it can be in the bulk in a vitreous form.

In order to study the possible influence of B-doping in the microstructure of the SrAl_2O_4 tridymite structure, a SAED and HREM study was performed. The SAED study corresponding to both samples, SrAl_2O_4 and $\text{SrAl}_{1.8}\text{B}_{0.2}\text{O}_4$, is in agreement with the tridymite unit cell proposed by XRD. Fig. 2 shows the SAED patterns along the [100], [010] and [001] zone axes for SrAl_2O_4 . No differences are observed in the B-doped sample.

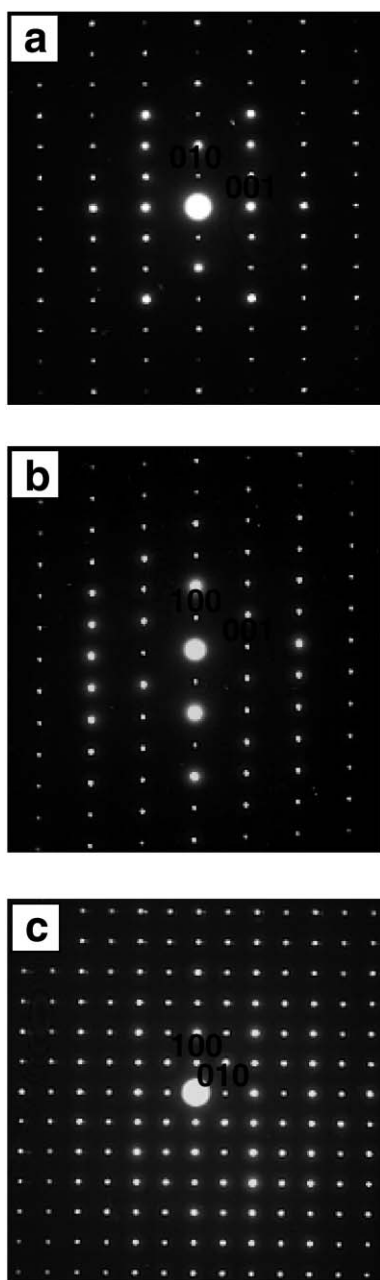


Fig. 2 SAED patterns corresponding to SrAl_2O_4 along (a) [100], (b) [010] and (c) [001] zone axes.

No impurities containing B were detected after checking around 100 crystals. These facts, together with XRD data, apparently suggest that boron has been randomly introduced into the tridymite structure.

Although HREM images are in agreement with the above unit cell, a more complex situation, due to the presence of defects, has been found. In fact, antiphase boundaries (APB) appear, either if boron is present or not, as can be observed in Figs. 3a and 4a, corresponding to both samples, SrAl_2O_4 and $\text{SrAl}_{1.8}\text{B}_{0.2}\text{O}_4$, along the [010] and [100] zone axes, respectively. As can be observed, a relatively low concentration of APB planar defects is randomly distributed along the crystal. In fact, the SAED pattern of the starting material does not show evidence of streaking due to the presence of isolated extended defects. However, streaking along b^* is clearly observed on the Fourier transform (FT) performed on an area of the crystal with relatively high concentration of APB, as seen in Fig. 3b. APB defects are also observed in the B-doped sample, but another kind of stacking fault not observed in the undoped SrAl_2O_4 material, indicated as "Z", is evident, as we will describe in the following.

The tridymite structure is kept in $\text{SrAl}_{1.8}\text{B}_{0.2}\text{O}_4$ in spite of the defects, as can be clearly observed along the [100] zone axis (Fig. 4a). Actually, a good agreement between experimental and calculated images ($\Delta t = 4$ and $\Delta f = -65 \text{ nm}$), having taken into account the atomic positions of SrAl_2O_4 ,³ is found, as seen in Fig. 4b. A projection of the structure is depicted in Fig. 4c.

On the other hand, a change in the contrast is observed in the APB-like defects with respect to that observed along both sides of the boundaries. Such a planar defect can be understood considering a shift of $1/2$ along b between both zones, as

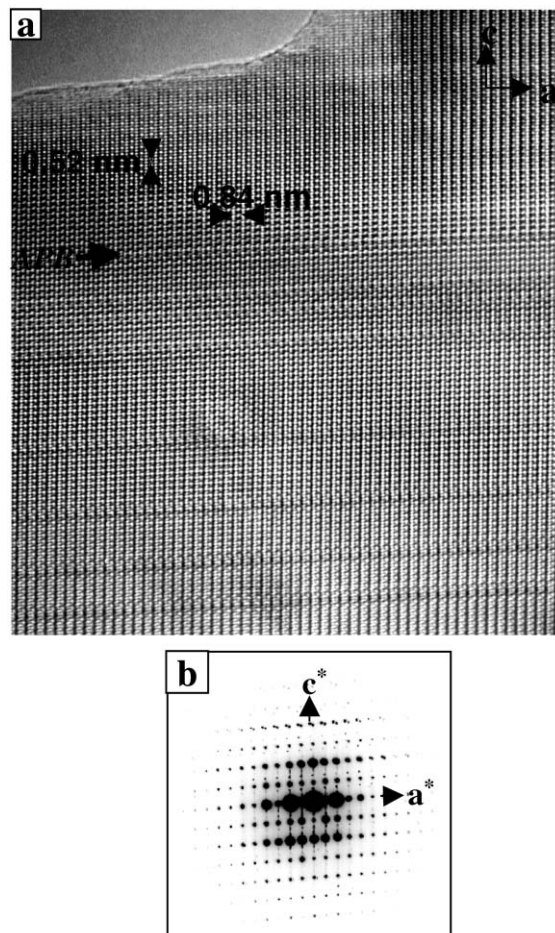


Fig. 3 (a) SrAl_2O_4 HREM image along [100] and (b) corresponding FT. The presence of APB is evident.

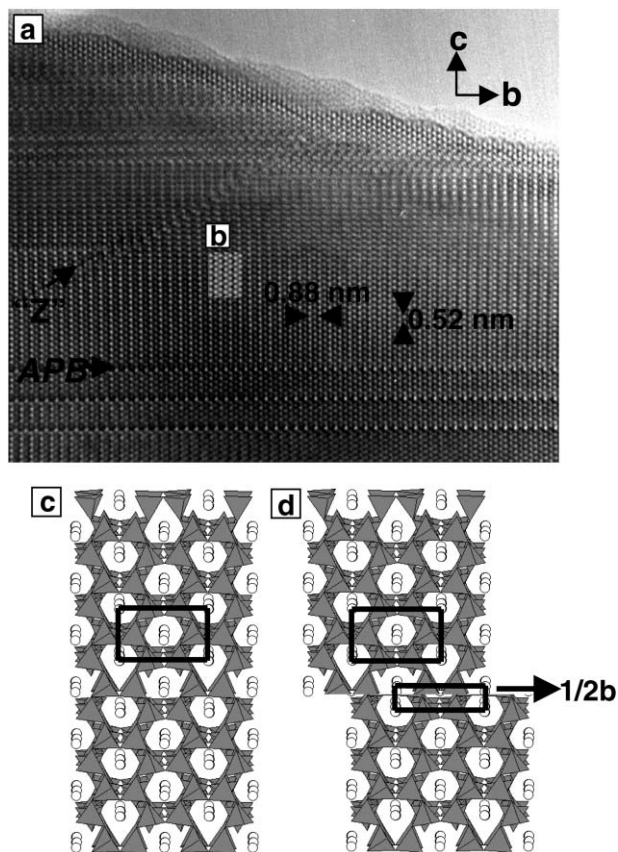


Fig. 4 (a) $\text{SrAl}_{1.8}\text{B}_{0.2}\text{O}_4$ HREM image along [100]. (b) Calculated image. (c) SrAl_2O_4 structure projected along [100]. (d) Same projection showing the displacement created by an APB-like defect.

represented in Fig. 4d, where it is observed that the discontinuity is indeed only produced over the junction of the two shifted areas. Furthermore, this seems to be a rich Sr zone. In this sense, it is well known that, under optimum defocus values, the darkest areas correspond to higher potential ones. In fact, black contrasts in the experimental image are placed along the APB. They must correspond to the higher atomic number element, *i.e.*, Sr, in agreement with the proposed structural model.

The new kind of defect only observed in the B-doped sample, (“Z”), also indicated in Fig. 4a, is similar to the so-called Z-type faulted dipole.⁹ Actually, it can be described as a plane separating two domains, structurally identical, but shifted by $1/2$ along b and by $1/2$ along c , *i.e.*, the planar fault is placed along the [011] direction. It is worth recalling that such defects are only formed in B-doped sample under the electron beam. At the very beginning, the material only shows APB. After some irradiation under the electron beam, the situation is suddenly modified by the formation of the new defect. A higher concentration of these faults can be observed in Fig. 5. Similar microstructural alterations have been previously described in silicon, where Z-type faulted dipoles are formed, again under the electron beam, when two dislocations interact with each other and connect through the stacking fault, giving rise to a Z shape.⁹

In our case, it seems reasonable to think that boron is pulling up from the structure due to the electron impact creating vacancies and then making possible a shifting of the crystallographic planes giving rise to the indicated defects along the [011] direction. In this sense, a stronger irradiation leads to another kind of defect. Fig. 6 is, again, an image along [100] and shows the presence of [011] twin planes (TP), leading to domains (A and B) rotated to each other by 60° . Note that, in this case, instead of the black contrast characteristic of the APB, both defects “Z” and “TP” exhibit white contrast, in

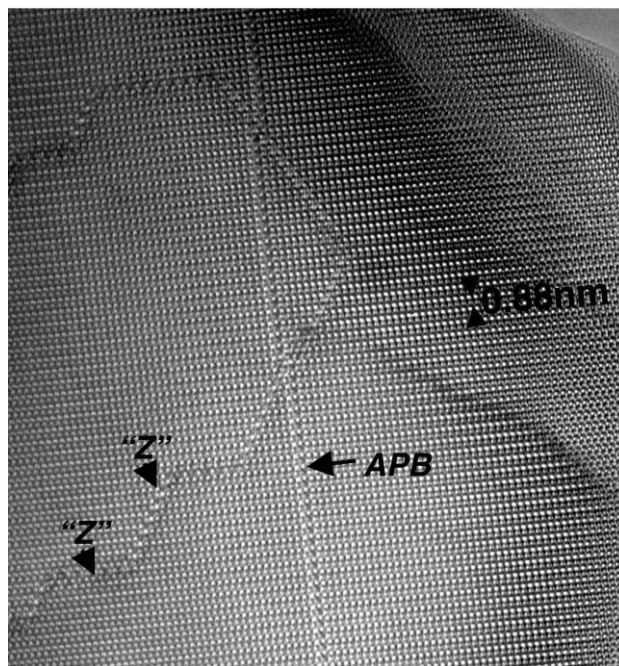


Fig. 5 HREM image of $\text{SrAl}_{1.8}\text{B}_{0.2}\text{O}_4$ along [100] showing a higher concentration of Z-type defects.

agreement with lower potential zones as indeed corresponding to the vacancies created, which originate from the elimination of boron. Such features are not observed in the undoped SrAl_2O_4 samples, which are stable under the electron beam.

The behaviour of the B-doped sample suggests that boron must substitute Al in $\text{SrAl}_{2-x}\text{B}_x\text{O}_4$. Since the boron concentration is relatively small, an ordered arrangement B–Al at the tetrahedral positions, is not expected, a random distribution being more likely. In fact, no superstructure has been detected. On the other hand, if boron was randomly arranged it would not be detected by HREM. In this sense, the defects created under the electron beam, “Z” and “TP”, seems to give

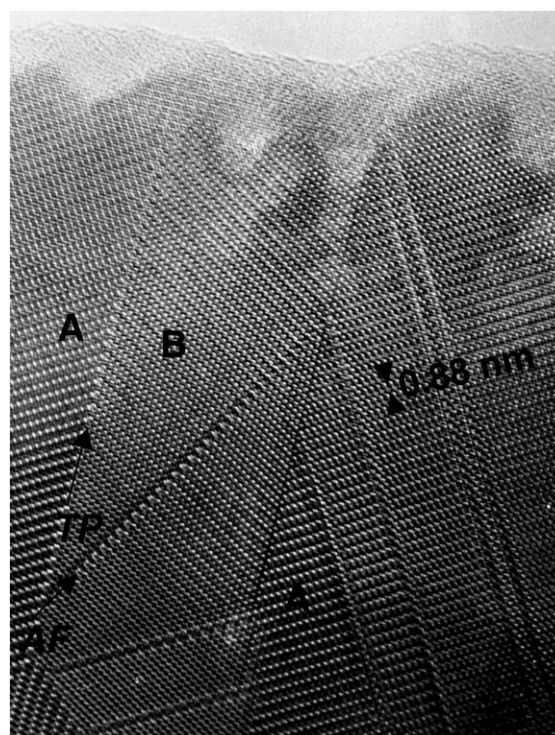


Fig. 6 HREM image of $\text{SrAl}_{1.8}\text{B}_{0.2}\text{O}_4$ along [100] showing TP and AF defects.

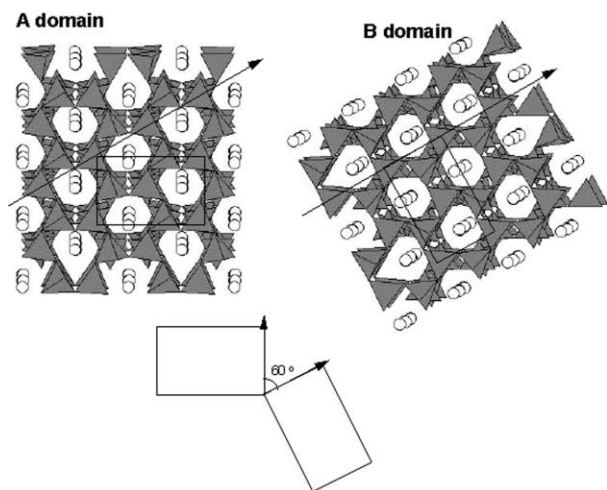


Fig. 7 Schematic representation of the twin domains originating after a 60° tilt.

valuable information about the boron distribution over the lattice. Therefore, since both defects only appear on the B-doped material after irradiation, they must be related to boron elimination. Moreover, if the defects created under the electron beam are arranged along [011], it can be assumed that boron is placed at the tetrahedral positions along this direction. On the other hand, as the B concentration is so small, substitution happens through randomly isolated planar defects over the crystal, as reflected in the experimental images.

Fig. 7 schematically represents how a tilt of 60° can be induced in the structure, leading to two differently oriented domains, when some hypothetical boron rows are eliminated. Domain A is represented in Fig. 7a. Fig. 7b corresponds to domain B obtained from A just by tilting 60° . As can be seen, both domains can be perfectly coupled.

Oxygen cooperative movements seem to be the driving force for these transitions, which have also been detected in quite different systems containing tetrahedral polyhedra, such as

$\text{Sr}_2\text{Co}_2\text{O}_5$,¹⁰ $\text{Sr}_2\text{CuGaO}_5$,¹¹ and LaBaCuGaO_y ,¹² brown millerite related oxides.

Conclusions

B-doping in tridymite-like SrAl_2O_4 drastically reduces the synthesis temperature for the ceramic route, opening new prospects for the use of $\text{SrAl}_{2-x}\text{B}_x\text{O}_4$ as a precursor for phosphor materials based on Eu-doped strontium aluminates. HREM shows that B atoms are placed in Al sites forming isolated planar defects along the [011] direction of the tridymite-type structure.

Acknowledgement

Financial support through research project 1FD1997-1198-C02-01(MAT) is acknowledged. We thank M. Fernanda Gazulla (Technologic Ceramic Institute, ITC, Universitat Jaume I, Castellón) for the ICP analyses.

References

- 1 H. Takasaki, S. Tanabe and T. Hanada, *J. Ceram. Soc. Jpn.*, 1995, **104**, 309.
- 2 V. Abbruscato, *J. Electrochem. Soc.*, 1971, **118**, 930.
- 3 A. R. Von Schulze and Hk. Müller-Buschbaum, *Z. Anorg. Allg. Chem.*, 1981, **475**, 205.
- 4 C. M. B. Henderson and D. Taylor, *Miner. Mag.*, 1982, **45**, 111.
- 5 S. Ito, S. Banno, K. Suzuki and M. Inagaki, *Z. Phys. Chem., Neue Folge*, 1977, **105**, 173.
- 6 T. Matsuzawa, Y. Aoki, N. Takeuchi and Y. Murayama, *J. Electrochem. Soc.*, 1996, **143**, 2670.
- 7 X-Ray powder data file, ASTM, JCPDS pattern 34-0379.
- 8 R. D. Shannon, *Acta Crystallogr., Sect. A*, 1976, **32**, 751.
- 9 D. Shindo and K. Hiraga, *High-Resolution Electron Microscopy for Materials Science*, Springer-Verlag, Tokyo, 1998.
- 10 J. M. González-Calbet and J. Rodríguez, *Inst. Phys. Conf. Ser.*, 1988, **93**(2), 379.
- 11 M. L. Ruiz-González, J. Alonso, C. Prieto, J. Ramírez-Castellanos and J. M. González-Calbet, *Chem. Mater.*, in press.
- 12 M. L. Ruiz-González, J. Ramírez-Castellanos and J. M. González-Calbet, *J. Solid State Chem.*, 2000, **155**, 372.